



PERGAMON

Solid State Communications 110 (1999) 375–379

solid
state
communications

Crystal field effects in the L_{23} XMCD of rare earth insulators

C. Neumann^a, B.W. Hoogenboom^b, A. Rogalev^a, J.B. Goedkoop^{a,*},[†]

^aEuropean Synchrotron Radiation Facility, B.P.: 220, F-38043 Grenoble, Switzerland

^bDPMC, Université de Genève, 24, quai Ernest-Ansermet, CH-1211 Genève 4, Switzerland

Received 9 December 1998; accepted 12 February 1999 by P. Dederichs

Abstract

We present the L_{23} XMCD of insulating rare earth (oxides and fluorides). The paramagnetic samples were magnetised in a 7 T field and cooled down to 5–10 K. We compare our XMCD data with a recent model for a $4f^N 5d^0$ electronic configuration. The L_2 edge displays a derivative shape, in agreement with the models. The L_3 edge however, is found to deviate, having a more complicated shape, due to the presence of quadrupolar contributions and, we argue, crystal field effects. © 1999 Elsevier Science Ltd. All rights reserved.

Keywords: A. Insulators; A. Magnetically ordered systems; D. Electronic states (localised); E. Synchrotron radiation; E. X-ray spectroscopy

1. Introduction

The electronic structure of rare-earth-containing materials is characterised by the dualism between the well localised, nearly atomic $4f$ shell, which is responsible for almost all of the magnetism of the rare earth ions, and the delocalised $5d$ and $6s$ shells that take part in the bonding. As direct overlap between the $4f$ shells on different sites is excluded, the interaction between the $4f$ magnetic moments has to be mediated by the delocalised states. Usually, this interaction is considered to include two parts: (i) the intra-atomic $5d$ – $4f$ exchange, described by atomic theory; and (ii) the inter-atomic hybridisation of the $5d$ shell with the surrounding atomic orbitals. The central issue for the description of the magnetism is the behaviour of the delocalised $5d$ shell, because it

couples the moment of the $4f$ shell to the surrounding magnetic environment.

After the first experimental observation of X-ray magnetic circular dichroism (XMCD) at the L_{23} ($2p \rightarrow 5d$) X-ray absorption edges of Gd-metal by Schütz et al. [1], it was expected that this spectroscopy would provide a useful tool for studying the $5d$ magnetic moment directly and separately from the $4f$ moment that is up to ten times stronger. While in principle this remains true today, it has been found that the description of the XMCD at the L-edges is rather complicated and the shape and amplitude cannot yet be explained by a single model.

Experiments so far have resulted in the following picture: the white line, that has mainly $2p \rightarrow 5d$ dipole character, shows strong dichroism, especially at the L_2 (L_3)-edge for the light (heavy) rare earth. Above the edge the XANES structure, related to dipolar transitions to the nd ($n > 5$) and unoccupied s states, shows XMCD that is 2–5 times smaller than the $5d$ contribution. An additional complication is the presence of quadrupolar transitions ($2p \rightarrow 4f$) that have been

* Corresponding author. Tel.: + 31-20-525-6362; fax: + 31-20-525-5102.

[†] Present address: University of Amsterdam, Valckenierstraat 65, NL 1018 XE, Amsterdam, Netherlands.

Table 1
Experimental details of the investigated samples

Sample	Type	Ordering temperature
CeF ₃	Single crystal (1% Ho)	Para
SmF ₃	Powder pellet	Para
Gd ₃ Ga ₅ O ₁₂ (GGG)	Single crystal	Ferri, T _c = 56 K
TbF ₃	Powder pellet	Ferro, T _c = 3.95 K
Dy ₂ O ₃	Powder pellet	Para
Er ₂ O ₃	Powder pellet	Antiferro, T _N = 4 K

identified at the pre-edge region of the L₃ edge. Such contributions were predicted early on by Carra and Altarelli [2] and Ebert et al. [3] and have subsequently been observed experimentally in many systems. Clear experimental proof of the quadrupolar nature of the L₃ XMCD has been obtained from the angular dependence of the XMCD at low temperatures [4]. Quadrupolar contributions were also isolated in X-ray resonant Raman experiments on the RFe₁₄B series [5,6] and much earlier in resonant X-ray magnetic scattering experiments [7]. Owing to the localised nature of the 4*f* states, the quadrupolar contributions can be simulated by theory. Such calculations have been used in attempts at simulating the spectra in combination with a bandstructure approach for the dipolar part [8–10]. Recently, atomic calculations for the line shape of the quadrupolar XMCD of all the rare earth elements have been published [11,12]. In the present article we show by the comparison of our data to these calculations that the quadrupolar and dipolar parts of the spectra are well separated in insulators.

XMCD experiments by Schütz et al. [13] and the LURE group [14,15] on the rare earth L-edges have shown that the description of the dipolar part of the L-edge XMCD, as it has been developed for the transition metals, breaks down. Especially the sum rules [8,16] have been found not to hold in this case. Apart from the quadrupoles discussed earlier, two other effects have been identified. As was pointed out first by Jo and Imada [17], the 4*f*–5*d* Coulomb interaction is strong and needs to be taken into account. In addition, it has been shown by Harmon and Freeman that the radial extent of the 5*d* wave functions depends on the spin [18]. This so-called breathing effect in turn leads to a spin-dependence of the 2*p*–5*d* matrix element which can change the spectra substantially [9,10].

Building on these ideas, recently we have developed [11,12,19] an atomic description based on a 5*d*⁰ Ansatz that takes into account the full atomic Coulomb interaction (including orbit–orbit interactions). This description led to new sum rules for the first moment of the derivative-like spectra in terms of the expectation value of the 4*f* shell operators (L_z, S_z and T_z). Inclusion of the spin-dependent radial wave function explains the transformation of derivative line shapes into single peaks and led to a good agreement with XMCD [15] and magnetic X-ray scattering [20] data of metallic systems, where breathing effects are thought to be important.

To test this model, we have investigated the XMCD of a number of rare earth insulators. Insulating systems have several advantages that simplify the problem: the rare earth ions are the only source of the magnetic properties, and the 5*d* shell is empty and very localised, implying that breathing effects should be absent. Our earlier work [19] dealt with rare earth elements in the middle of the series. In this article we present new data on insulators of lighter and heavier rare earth elements. Particularly the light systems are difficult to study because they have only small paramagnetic moment, making it difficult to saturate the systems. We find that while the L₂ XMCD behaves as predicted by the 5*d*⁰ model that we presented earlier [11,12], the L₃ line shapes are more complicated. Possible reasons for this breakdown of the model are discussed.

2. Experimental details and results

The experiments reported here have been carried out at the ESRF beamline ID12A. The second harmonic of the helical undulator Helios 2 was used and the first harmonic was systematically cut off upstream from the monochromator using a 125 μm graphite foil. The circular polarisation rate beyond the Si(111) monochromator is estimated to be 88% at the Ce L-edge, 90% at the Tb edge and 92% at the Er edge.

The samples were prepared from powder pellets diluted with boron nitride powder or from single crystals (see Table 1 for experimental details). Samples were mounted on an Al sample holder that could be screwed tightly on a liquid helium flow cryostat

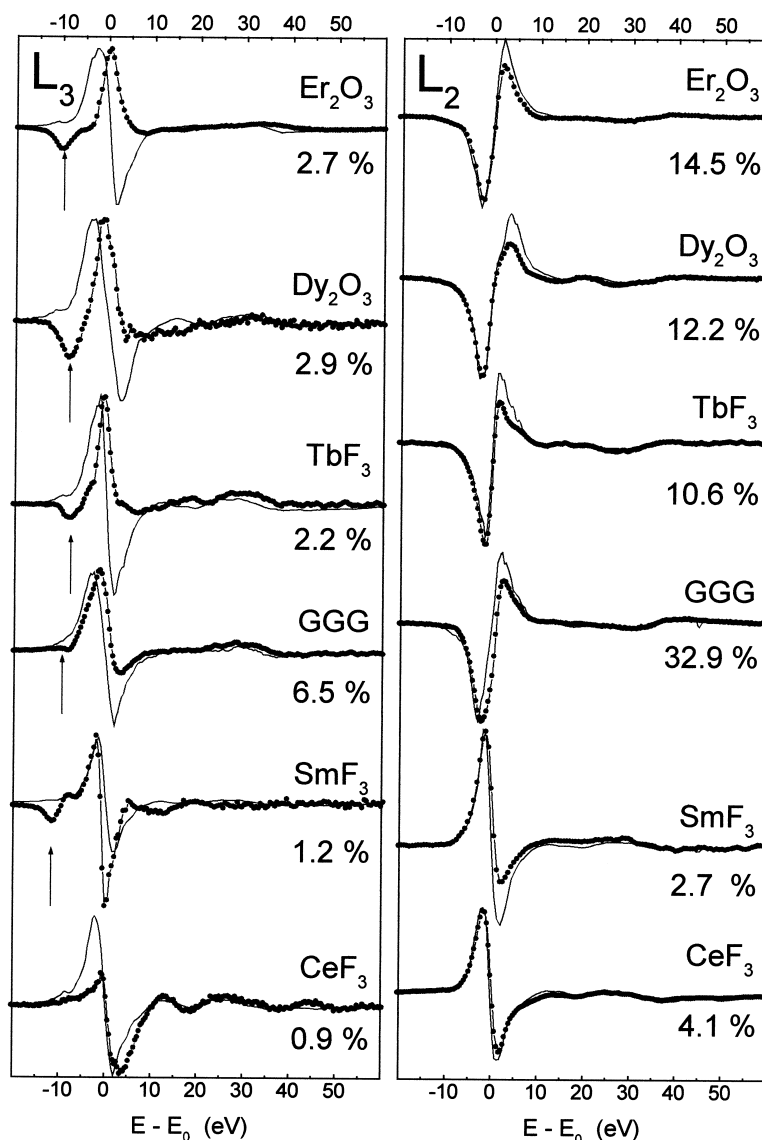


Fig. 1. XMCD spectra (full line) in comparison with the derivative (dotted line) of the spin-averaged XAS spectra. In addition, the peak-to-peak amplitude of the XMCD is given. The arrows indicate the position of the pre-edge structure, which is assigned to the quadrupolar contributions in the L_3 XMCD.

inserted into a 7 T split-coil superconducting magnet. As a result of the problem of controlling the thermal coupling to the sample surface, especially of the powder samples, the actual temperature cannot be estimated precisely. Calibration measurements indicate 5–10 K as reasonable estimates but are not accurate enough to give a precise value of the magnetic

saturation. The samples were magnetised along the beam direction. The sample surfaces were mounted at 45° to the incident light direction and fluorescence radiation was collected with a Si photodiode mounted at 90° which is completely insensitive to the magnetic field.

Fig. 1 shows the XMCD spectra of the samples

Table 2

XMCD peak intensities scaled to the intensity of the corresponding edge jump (normalised to the core hole degeneracy) and L_3 quadrupole positions with respect to the absorption maximum

Sample	XMCD intensity		Quadrupole position (eV)
	L_3 (%)	L_2 (%)	
CeF ₃	0.9	4.1	n.a.
SmF ₃	1.6	2.7	– 11.5
GGG	6.5	32.9	– 8.5
TbF ₃	2.2	10.6	– 7.6
Dy ₂ O ₃	2.9	12.2	– 8.4
Er ₂ O ₃	2.7	12.9	– 9.8

listed in Table 1. The spectra are represented normalised to the core hole degeneracy (4 and 2, respectively). All spectra shown are the average of 6–12 scans. In cases where the XMCD signal was very weak, notably at the L_3 edges of Ce and Sm, the data had to be recovered by averaging of the spectra after taking out the pre-edge intensity and normalisation of the post-edge intensity at ~ 100 eV above the edge. The spectra were corrected for fluorescence saturation effects using a homographic transform [21]. The reproducibility was checked in a number of cases using different combinations of field and helicity flipping, which yielded the correct inversion of the spectra. The energy scales were aligned to the peak of the spin-averaged XAS spectra for ease of comparison.

In Fig. 1 the XMCD-spectra are compared to the derivatives of the spin-averaged XAS spectra. The latter curves are scaled by an arbitrary factor to the maximum (L_3) or minimum (L_2) of the XMCD. The arrows indicate the position of the quadrupolar contributions. In addition, the peak-to-peak amplitude of the XMCD is given, corrected for self-absorption and beam polarisation. Note that, as we do not know the magnetic saturation, these values are indicative only. Table 2 shows the XMCD peak-to-peak amplitude and the energy positions of the L_3 quadrupole features indicated by the arrows in Fig. 1 with respect to the white line maximum.

3. Discussion

The right panel of Fig. 1 shows that the L_2 XMCD spectra have line shapes that are close to the derivative

of the XAS. The sign of the spectra inverses between the light and heavy rare earths, as expected. The correspondence between the XMCD and derivative curves seems particularly good at the beginning and the end of the series, Ce and Er, in accordance with the model for $5d^0$ systems. Even the XANES oscillations are seen to have derivative-like XMCD. However, in the middle of the series the intensity of the second peak of the XMCD is much smaller in comparison with the derivative curve.

The situation is more complicated at the L_3 edge. While the Ce, Sm and Gd spectra still have some resemblance with the derivative curve, for the heavier end of the series all agreement is lost. On the low energy side, this is clearly due to the quadrupolar transitions, which for Gd, Tb, Dy and Er are quite strong and can already be identified in the XAS in the form of a shoulder (not shown), or equivalently, in the derivative curves of Fig. 1. In the XMCD the quadrupoles show up as a negative peak (indicated by arrows in Fig. 1) for Er, Dy, Tb and possibly Gd, and as a dispersive structure for Sm. The shapes and positions of these features agree quite well with published calculations [22]. By comparison with these calculations one arrives at the important conclusion that in these insulating materials the quadrupolar contributions are well separated from the main L_3 dipolar XMCD, and cannot explain the deviation from simple derivative line shapes. The single-peak line shapes of the dipolar L_3 XMCD must therefore have a different origin.

We rule out an explanation in terms of spin-dependence of the $5d$ orbital wavefunction [9,10]. This effect needs hybridisation: it occurs in metals, but in insulators the $5d$ band is too localised to allow for much difference in the $5d$ radial extend between spin-up and spin-down states. Another possible origin of the deviating behaviour could be $5d$ crystal field effects, which are well known to be present in the L_{23} XAS of $3d$ and $4d$ [23–25]. Such splitting should also be present in the rare earth $5d$ edges but are masked by the lifetime broadening. Splittings of the order of 3.5 eV have recently been recovered in Er₂O₃ by deconvolution of the lifetime broadening [26]. As the heavy rare earth oxides all have the Mn₂O₃ structure we expect similar splitting in all of them unless interactions with the $4f$ shell are important.

De Groot et al. [25] already noticed that in $4d$

transition metals crystal-field effects split up the L_3 edge more than the L_2 edge. In preliminary crystal-field calculations for La we find that such differences between the edges are relatively small for the $5d$ series when the $4f$ shell is empty. However, a calculation for Ce (one $4f$ electron) shows that the presence of a $4f$ electron causes a substantial splitting of the L_3 edge but not on the L_2 . Therefore it is very likely that crystal field splittings are responsible for the deviation of the L_3 XMCD from the simple derivative shape. We suspect the origin of this effect lies in the different multipole interactions between the $2p_{3/2}$ and $2p_{1/2}$ core holes with the valence state multipole.

4. Conclusion

We have presented L_{23} XMCD data on insulating rare earth systems covering the light- and heavy rare earth elements. The L_2 edge is found to behave close to as expected from a $5d^0$ Ansatz. In contrast, the L_3 edge XMCD is found to be more complicated in structure. In part this is due to well-resolved quadrupolar contributions, but these can be separated out by comparison to atomic calculations. The deviation of the dipolar part from the $5d^0$ model is very likely due to crystal field interactions that work stronger on the L_3 than on the L_2 edge. Although preliminary calculations point in the direction of crystal fields as being the source of the deviation of the L_3 edge from the simple derivative behaviour, further work is necessary to elucidate this point.

References

- [1] G. Schütz, W. Wagner, W. Wilhelm, P. Kienle, R. Zeller, R. Frahm, G. Materlik, Phys. Rev. Lett. 58 (1987) 737.
- [2] P. Carra, M. Altarelli, Phys. Rev. Lett. 64 (1990) 1286.
- [3] H. Ebert, G. Schütz, W.M. Temmerman, Sol. State Comm. 76 (1990) 475.
- [4] J.C. Lang, G. Srajer, C. Detlefs, A.I. Goldman, H. König, X. Wang, B.N. Harmon, R.W. McCallum, Phys. Rev. Lett. 74 (1995) 4935.
- [5] M.H. Krisch, C.C. Kao, F. Sette, W.A. Caliebe, K. Hamalainen, J.B. Hastings, Phys. Rev. Lett. 74 (1995) 4931.
- [6] F. Bartolomé, J.M. Tonnerre, L. Sève, D. Raoux, J. Chaboy, L.M. García, M. Krisch, C.C. Kao, Phys. Rev. Lett. 79 (1997) 3775.
- [7] D. Gibbs, D.R. Harshman, E.D. Isaacs, D.B. McWhan, D. Mills, C. Vettier, Phys. Rev. Lett. 61 (1988) 1241.
- [8] P. Carra, B.T. Thole, M. Altarelli, X. Wang, Phys. Rev. Lett. 70 (1993) 694.
- [9] X. Wang, T.C. Leung, B.N. Harmon, P. Carra, Phys. Rev. B 47 (1993) 9087.
- [10] X. Wang, V.P. Andropov, B.N. Harmon, J.C. Lang, A.I. Goldman, J. Appl. Phys. 75 (1994) 6366.
- [11] M. van Veenendaal, J.B. Goedkoop, B.T. Thole, Phys. Rev. Lett. 78 (1997) 1162.
- [12] M. van Veenendaal, J.B. Goedkoop, B.T. Thole, J. Electr. Spectr. Rel. Phenom. 86 (1997) 151.
- [13] G. Schütz, M. Knulle, H. Ebert, Physica Scripta T (1993) 302.
- [14] F. Baudelet, C. Giorgetti, S. Pizzini, C. Brouder, E. Dartyge, A. Fontaine, J.P. Kappler, G. Krill, J. Electr. Spectr. Rel. Phenom. 62 (1993) 153.
- [15] C. Giorgetti, PhD thesis, Université Paris-Sud, Orsay, 1994.
- [16] B.T. Thole, C. Paolo, F. Sette, G. van der Laan, Phys. Rev. Lett. 68 (1992) 1943.
- [17] T. Jo, S. Imada, J. Phys. Soc. Japan 62 (1993) 3721.
- [18] B. Harmon, A. Freeman, J. Phys. Rev. B 10 (1974) 1979.
- [19] J.B. Goedkoop, A. Rogalev, M. Rogaleva, C. Neumann, J. Goulon, M. van Veenendaal, B.T. Thole, J. Phys. IV France 7 C2 (1997) 397.
- [20] J.P. Hill, A. Vigliante, D. Gibbs, J.L. Peng, R.L. Greene, Phys. Rev. B 52 (1995) 6575.
- [21] J. Goulon, C. Goulon-Ginet, R. Cortes, J.M. Dubois, J. Physique 43 (1982) 539.
- [22] M. van Veenendaal, R. Benoist, Phys. Rev. B 58 (1998) 3741.
- [23] F.M.F. de Groot, J.C. Fuggle, B.T. Thole, G.A. Sawatzky, Phys. Rev. B 42 (1990) 5459.
- [24] F.M.F. de Groot, J.C. Fuggle, B.T. Thole, G.A. Sawatzky, Phys. Rev. B 41 (1990) 928.
- [25] F.M.F. de Groot, Z.H. Hu, M.F. Lopez, G. Kaindl, F. Guillot, M. Trone, J. Chem. Phys. 101 (1994) 6570.
- [26] P. Loeffen, R.F. Pettifer, S. Müllender, M. van Veenendaal, J. Röhrler, D.S. Sivia, Phys. Rev. B 54 (1996) 14877.